

Progress Report

**"Title: Bay of Bengal as the Gateway to Indian Monsoon at Intraseasonal Time-
.....scales: A Regional Coupled Model Study**

PI: Raghu Murtugudde
Earth System Science Interdisciplinary Center, University of Maryland
College Park, MD 20742

Period for this report: Mar 1st, 2013 - Aug 31st, 2013

0. Synergistic activities

The PI continued his subseasonal variability research on multiple fronts with related fundings. The continued ONR funding will allow synergistic progress on these fronts to advance the process and predictive understanding on MJO predictions along with MISO and Monsoon predictions also.

1. Zhou, L., and R. Murtugudde, 2013: Impact of Northward-Propagating Intraseasonal Variability on the onset of Indian summer monsoon. *J. Clim.*, In press.
2. Valsala, V., Y.K. Tiwari, P. Pillai, M. Roxy, S. Maksyutov, and R. Murtugudde, 2013: Intraseasonal variability of terrestrial biospheric CO₂ fluxes over India during summer monsoons. *J. Geophys. Res. Biogeosci.*, **118**, 752-769, doi:10.1002/jgrg.20037.
3. Ganeshan, M., R. Murtugudde, and J. Strack, 2012: The role of negative buoyancy in surface-based convection and its representation in cumulus parameterization schemes. In pres, *J. Appl. Meteorol. Climatol.*
4. Ganeshan, M., R. Murtugudde, and M. Imhoff, 2013: The UHI-Induced warm season rainfall modification in propagating and non-propagating storms. *Urban Climat*, In press.

1. Abstract

It has been widely accepted that air-sea interaction plays an important role in monsoon intraseasonal oscillation (MISO), particularly for convections propagating northward in the Bay of Bengal (BoB). In this study, we performed coupled modeling simulations of MISO with regional atmospheric and oceanic models, specifically "Weather Research and Forecasting Model (WRF)" and "Regional Ocean Modeling System (ROMS)." By enabling coupling, compared to the same WRF run with prescribed SST forcing, we found notable improvements; e.g., the precipitation signals become

sharper and clearer with increased magnitude of precipitation, and observation-like temporarily southward propagating features are detected along 90°E longitude. We also tried to compare the effect of ocean resolution (0.5°x0.5° vs. 0.125°x0.125°) on the precipitation simulation. In our results, the finer resolution of ocean model didn't result in notable differences from coarser one while it made the coupled system much more unstable.

2. Experimental Setup and Observation Data

We employed WRF as an atmospheric numerical model. On the domain of BoB (77°-99°E, 6°-28°N), we ran WRF with boundary conditions obtained from NCEP FNL Operational Global Analysis DATA (1°x1°, 6-hourly) and Hi-resolution (12km) GHRSSST (6-hourly) for the control run (= prescribed run). The WRF is famous for thousands of combinations of physical schemes available. For simplicity, we followed NCAR's real-time hurricane run setting in 2012 as shown in Table 1.

Table 1. List of employed schemes in WRF simulation

Microphysics	WRF single-Moment 6-class scheme
Long- and short-wave radiation	RRTMG scheme
Surface and Land	MM5 and Noah Land surface model
PBL	Yonsei-University Scheme
Cumulus	Tiedtke scheme (Univ. of Hawaii version)
Shallow Convection	Not implemented

We used ROMS as an oceanic partner. We set up an exactly same domain as the one of WRF, and tested two different horizontal resolutions, 0.5°x0.5° vs. 0.125°x0.125°. Since the BoB is closed to West, North, and East in our domain, boundary conditions from the NCEP Global Ocean Data Assimilation System (GODAS) monthly data are only set at the southern boundary.

Simply speaking, coupling was enabled by providing SST from ROMS to WRF, and surface wind and wind stress, heat and moisture flux, and shortwave flux for K-profile parameterization (Large et al. 1994) are provided from WRF to ROMS. For the 0.5° ROMS, we performed 3-hourly coupling, i.e., 3-hour mean atmospheric variables are transferred to ROMS, and the SST result of ROMS 3-hour run is provided to WRF. This setting worked for entire 20-day target period (see below) simulation. In the case of 0.125° ROMS simulation, we tested 45-min, 60-min, and 90-min coupling, but all experiments blew up after 9-12 days.

The selected target period for this study is from June 01, 2011 to June 20, 2011. According to the Bimodal ISO index (Kikuchi et al., 2011), this period corresponds to phases 4 to 6 with stronger than normal magnitude. TRMM precipitation data shows that precipitation is detected around 10°N during June 3-5, and notable core of precipitation becomes mature during June 15-17 at the northern tip of BoB (Fig. 1). In addition, we also examined temporal evolution of precipitation along 90°E (Fig. 2). As shown in Sahany et al. (2010), the precipitation pattern shows several events of temporary southward propagation in latitudes 6°N to 20°N (June 3rd-15th).

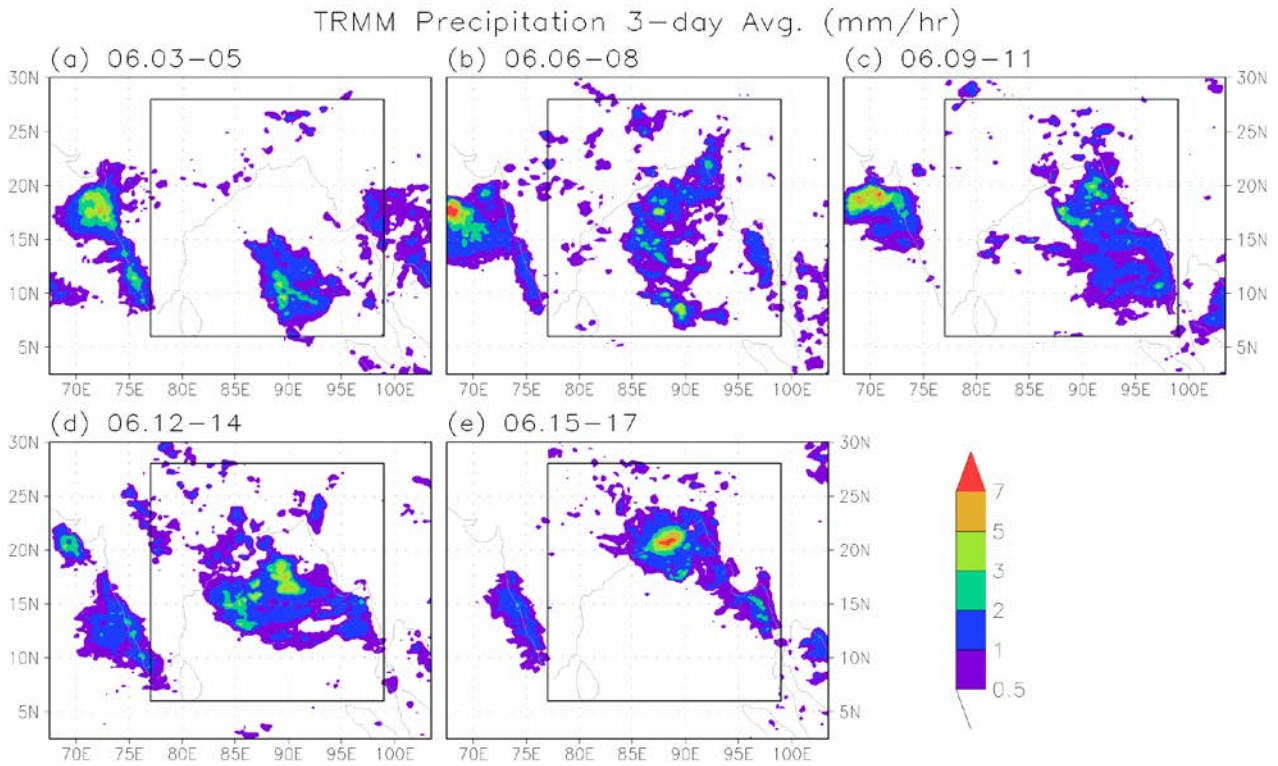


Figure 1. TRMM precipitation 3-day average from (a) June 3-5 to (e) June 15-17. Inner box indicates the domain of numerical simulations.

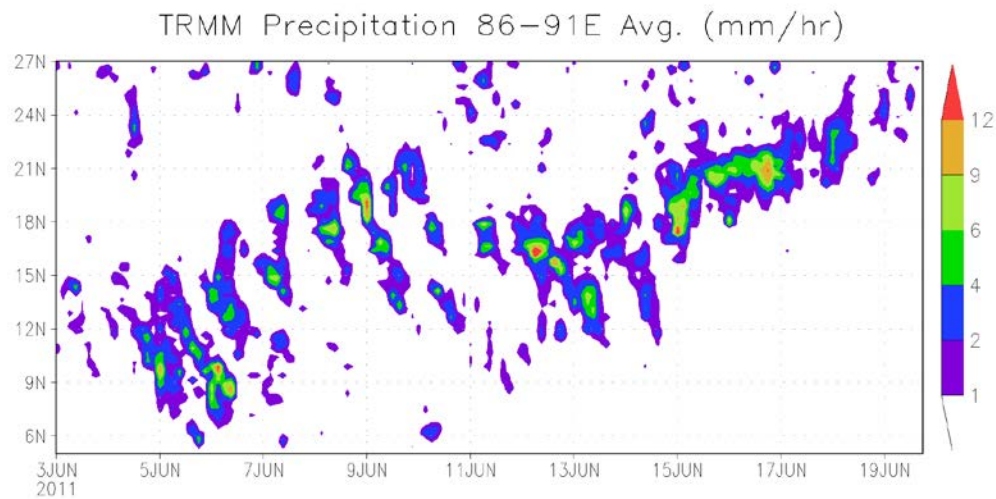


Figure 2. TRMM precipitation zonal mean from 86°-91°E.

3. WRF-only and WRF-ROMS coupled simulation results

are notably improved in the coupled simulations. In Fig. 7, the temporary southward propagating pattern in first 10 days is clearer in the 0.5° ROMS coupled WRF. This feature is even more manifest with details in the finer resolution ROMS coupled WRF (Fig. 8), which is partly due to more frequently available outputs in the case of 0.125° ROMS (1 hour vs. 3 hour). Of course, the heavy precipitation during June 15th to 17th is another notable improvement of coupled simulation compared to WRF-only simulation.

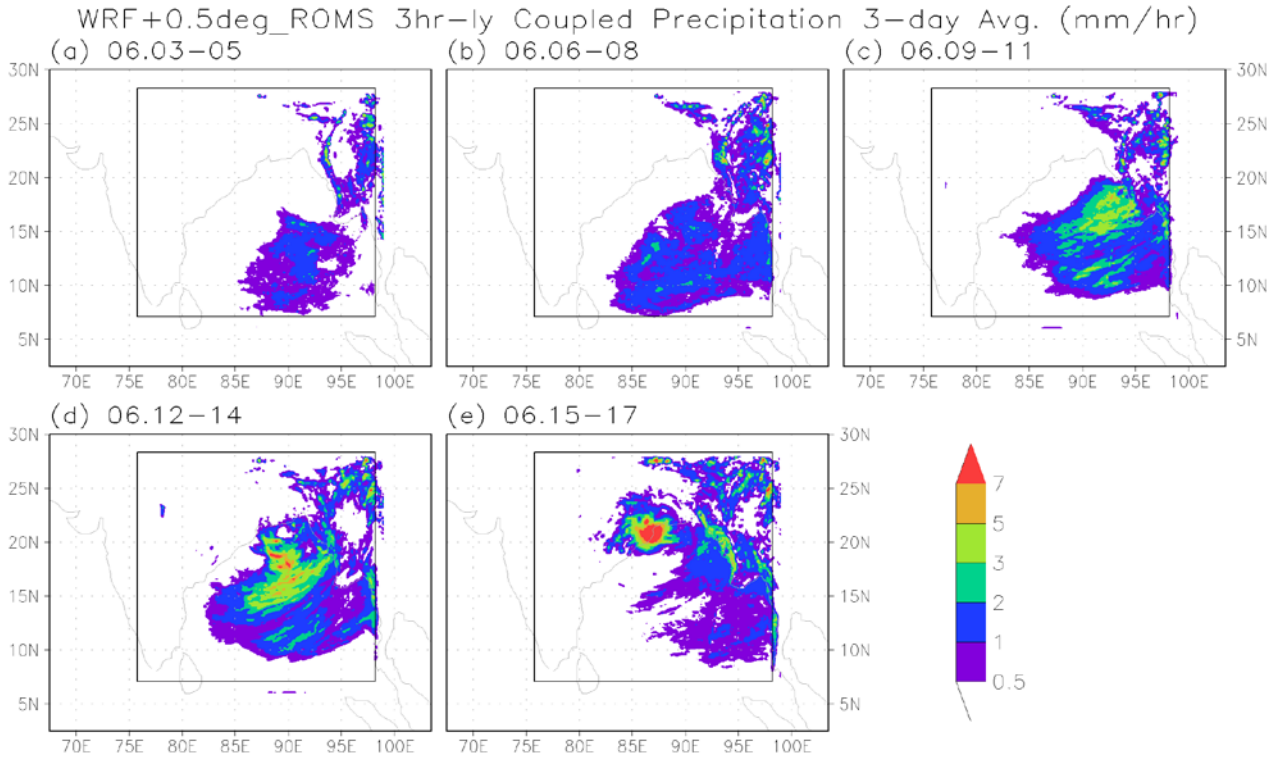


Figure 4. Same as Fig. 1, but for the results of 3-hourly coupling between WRF and 0.5° resolution ROMS.

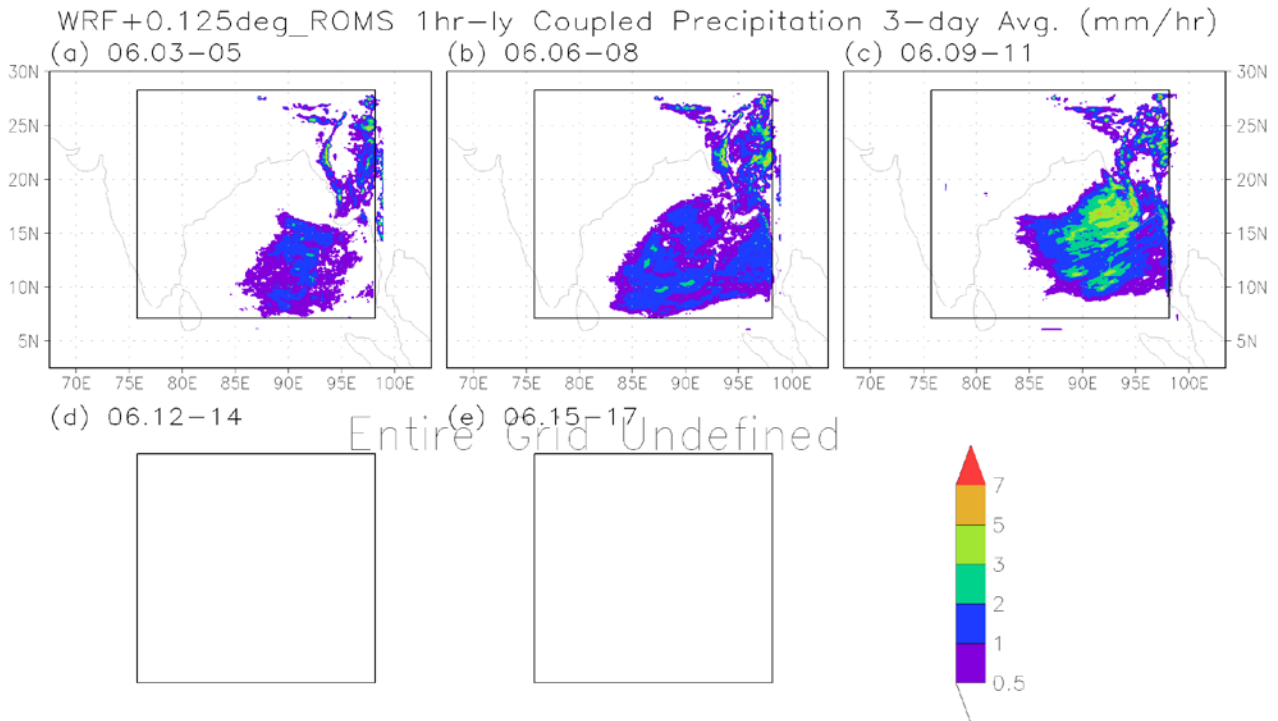


Figure 5. Same as Fig. 1, but for the results of 1-hourly coupling between WRF and 0.125° resolution ROMS. These results are only available to June 11th due to unstable blowing-up.

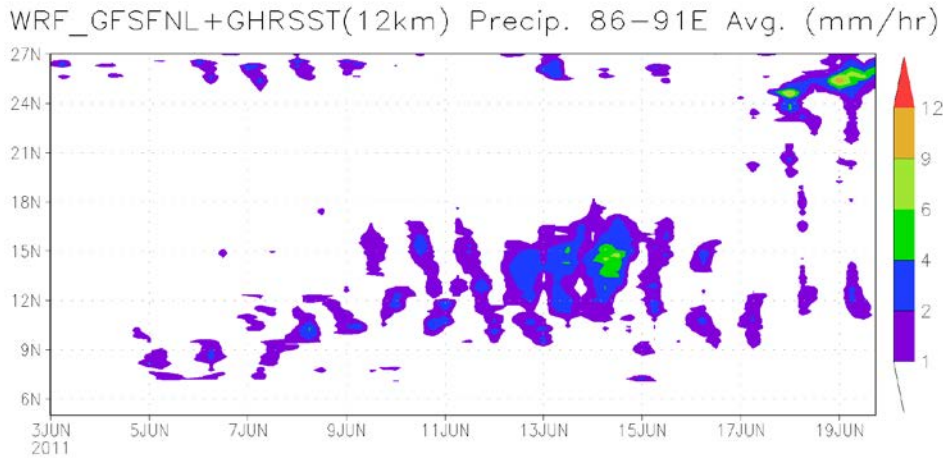


Figure 6. Same as Fig. 2, but for the results of WRF simulation forced by prescribed SST.

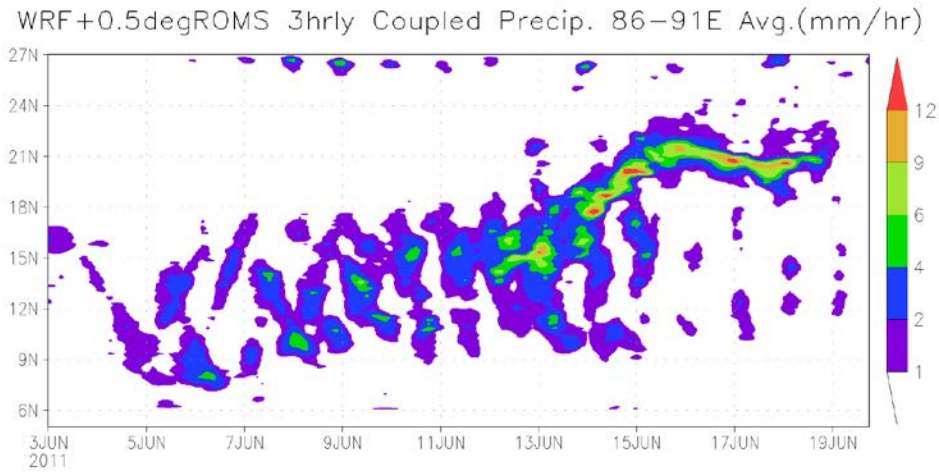


Figure 7. Same as Fig. 2, but for the results of 3-hourly coupling between WRF and 0.5° resolution ROMS.

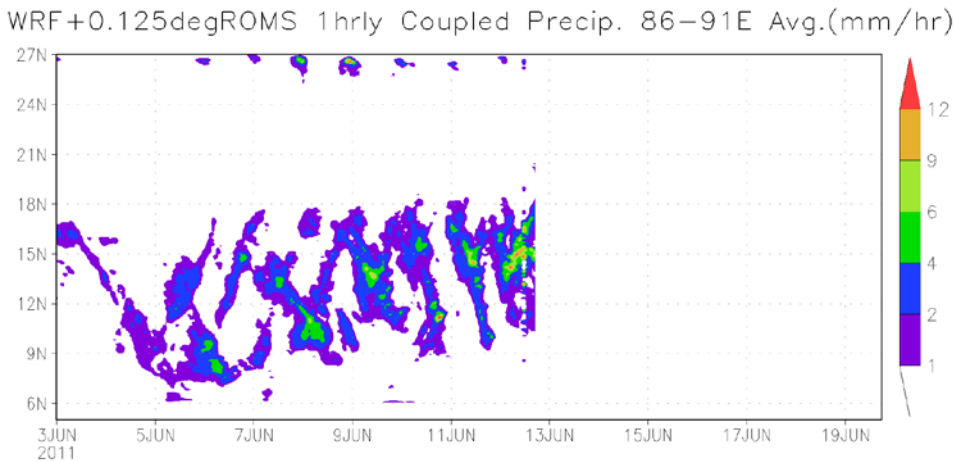


Figure 8. Same as Fig. 2, but for the results of 1-hourly coupling between WRF and 0.125° resolution ROMS.

Lastly, in order to examine the effect of ROMS resolution on the coupled simulation, we calculated model SST deviations from observation. We examined temporal evolution of area averaged model error over the model domain (Fig. 9) and the time average of model error (Fig. 10). These results indicate that the ocean model resolution and coupling time hardly influence the model performance of SST simulation. In Fig. 10, for the same time span (June 1st-12th), model errors compared to observed SST are nearly indistinguishable between two different settings of ROMS model. However, we think it is too early to conclude that a finer resolution ocean model is unnecessary to simulate Indian monsoon. This is because we believe that the finer resolution ocean model can be further improved by more details of boundary conditions, e.g., riverine fresh water input.

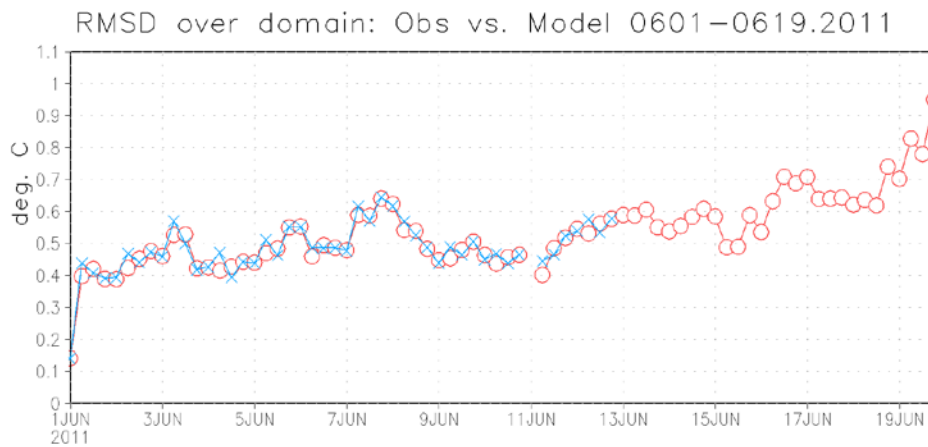


Figure 9. Model domain mean of root-mean-squared-difference between observed and simulated SST. Red circle indicates the results of WRF + 0.5° resolution ROMS run, and blue x indicates the results of WRF + 0.125° resolution ROMS run.

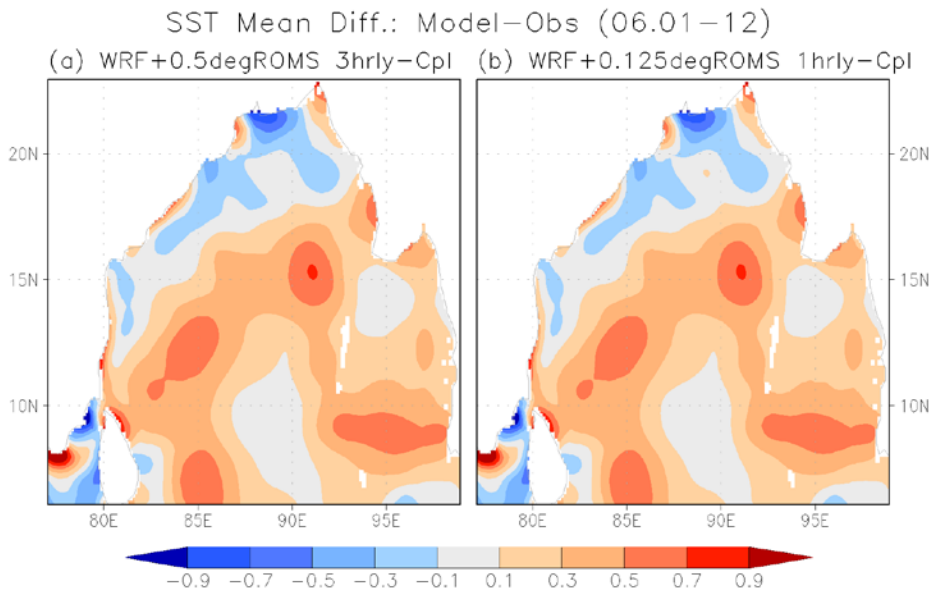


Figure 10. SST mean difference, model SST – observed SST for the period from June 1st to 12th. (a) WRF + 0.5° resolution ROMS run and (b) WRF + 0.125° resolution ROMS run.

References

- Kikuchi, K., B. Wang, and Y. Kajikawa, 2011: Bimodal representation of the tropical intraseasonal oscillation. *Clim. Dyn.*, **38**, 2989-2000. doi:10.1007/s00382-011-1159-1.
- Large, W. G., J. C. McWilliams, and S. C. Doney, 1994: Oceanic vertical mixing: a review and a model with a nonlocal boundary layer parameterization. *Rev. Geophys.*, **32**, 363-403.
- Sahany, S., V. Venugopal, and R. S. Nanjundiah, 2010: Diurnal-scale signatures of monsoon rainfall over the Indian region from TRMM satellite observations. *J. Geophys. Res.*, **115**, D02103, doi: 10.1029/2009JD012644.